Reactivity of unactivated peroxymonosulfate with nitrogenous compounds

Maolida Nihemaiti, Ratish Ramyad Permala, Jean-Philippe Croué

Reactivity of Unactivated Peroxymonosulfate with Nitrogenous Compounds

Maolida Nihemaiti [a, b], Ratish Ramyad Permala [c], Jean-Philippe Croué [a, d, *]

[a] Curtin Water Quality Research Centre, School of Molecular and Life Sciences, Curtin University, GPO Box U1987, Perth WA 6845, Australia

[b] LEESU (UMR MA 102), Université Paris-Est - AgroParisTech, 61 Avenue du Général de Gaulle, 94010 Créteil Cedex, France

[c] School of Pharmacy and Biomedical Science, Curtin University, GPO Box U1987, Perth WA 6845, Australia

[d] Institut de Chimie des Milieux et des Matériaux IC2MP UMR 7285 CNRS, Université de Poitiers, France

Corresponding Author

*Tel.:+33(0)787094466; e-mail: jean.philippe.croue@univ-poitiers.fr

Abstract

A recent investigation has demonstrated that peroxymonosulfate (PMS), a peroxide commonly applied as a radical precursor during advanced oxidation processes (AOPs), can degrade organic contaminants without the involvement of radicals. However, little is known about this non-radical reaction mechanism. In this study, the reactivity of PMS with several nitrogenous compounds was investigated. Fluoroquinolone antibiotics (except for flumequine) were rapidly degraded by direct PMS oxidation, followed by aliphatic amines (e.g., metoprolol and venlafaxine) and nitrogenous heterocyclic compounds (e.g., adenine and caffeine) at pH 8. The degradation rate of fluoroquinolones followed a second-order kinetic and was highly pH and structure-dependent. Unlike the radical-based AOPs, the direct degradation of contaminants by PMS was less influenced by the scavenging effect of the water matrix. High-Resolution Mass Spectrometry (HRMS) analysis demonstrated that the piperazine ring of fluoroquinolones was the main reaction site. Results showed that the direct electron-transfer from nitrogenous moieties (piperazine ring) to PMS can produce amide and aldehyde compounds. An amide-containing transformation product of ciprofloxacin (*m/z* 320), showing the highest signal intensity on HRMS, was previously recorded during ozonation. Moreover, the hydroxylamine analogue of ciprofloxacin and enrofloxacin *N*-oxide were tentatively identified, and the formation of the latter was not impacted by the dissolved oxygen in water. These results suggested that PMS also reacts with nitrogenous compounds via oxygen transfer pathway. Agar disk-diffusion tests indicated that PMS treatment efficiently removed the antibacterial activity of ciprofloxacin with the complete degradation of parent antibiotic, except for the transformation products in an earlier stage, which might still exert antibacterial potency.

Keywords

Peroxymonosulfate, nitrogenous compounds, high-resolution mass spectrometry, reaction mechanism

Abbreviations

AOPs	Advanced Oxidation Processes
CIP	Ciprofloxacin
D	Distribution Coefficient
E. coli B	*Escherichia. Coli* B
ENR	Enrofloxacin
HPLC	High-Performance Liquid Chromatography
HRMS	High-Resolution Mass Spectrometry
LC	Liquid Chromatography
NOM	Natural Organic Matter
PDS	Peroxydisulfate
PMS	Peroxymonosulfate

1. Introduction

Advanced Oxidation Processes (AOPs) have gained increasing interest in recent years for the removal of refractory contaminants during water treatment and soil remediation. Hydrogen peroxide (H_2O_2), peroxydisulfate ($S_2O_8^{2-}$, PDS), and peroxymonosulfate (HSO_5^-, PMS) are the commonly used peroxides for AOPs. The activation of these peroxides by energy (e.g., UV irradiation) and electron transfer (e.g., transition metal-based catalysis) generates strong oxidizing species such as hydroxyl radical ($^{\bullet}OH$, 1.9–2.7 V) and sulfate radical ($SO_4^{\bullet-}$, 2.5–3.1 V) (Neta et al., 1988). Many studies have demonstrated that $^{\bullet}OH$ and $SO_4^{\bullet-}$ have high potential to eliminate pharmaceuticals, pesticides, and industrial contaminants (Lutze et al., 2015; Wols et al., 2015). However, certain water matrix components (e.g., organic matter, bicarbonate, and halides) are known to reduce the efficiency of AOPs by significantly scavenging the radicals (Zhang et al., 2013; Yang et al., 2016b). Moreover, the leaching of heavy metal (e.g., cobalt) can be an important issue during transition metal-based AOPs (Ike et al., 2018).

PMS is commercially available and known as Oxone ($2KHSO_5.\ KHSO_4.\ K_2SO_4$). It is relatively stable, thus convenient for storage and transportation. PMS has been applied as a non-chlorine disinfectant in swimming pools and for delignification in paper and pulp industry. The electron-transfer from transition metal-based catalysts (e.g., cobalt, copper, iron) and the cleavage of peroxide bond in PMS by UV irradiation and ultrasound can generate $SO_4^{\bullet-}$ and $^{\bullet}OH$ (Ghanbari and Moradi, 2017).

It has been recently reported that organic contaminants (e.g., carbamazepine, sulfamethoxazole, chlorophenol) can be decomposed by direct PMS oxidation (i.e., no radical initiator). Quenching studies and electron paramagnetic resonance spectrometry analysis confirmed that contaminant transformation was attributed to the direct oxidation by PMS without the contribution of radicals (Yang et al., 2018). However, little is known about the

77 reaction mechanism of this non-radical process. Previous studies have reported that sulfur-
78 containing compounds (thioether sulfur of β-lactam antibiotics) can be substituted by the
79 oxygen from PMS to produce sulfoxide products (Chen et al., 2018). However, the oxygen
80 substitution pathway can be affected by steric hindrance, especially for contaminants with
81 complex structures (Chen et al., 2018).
82 PMS is a strong electron-acceptor with redox potential (E^0 (HSO_5^-/HSO_4^{2-}) =1.82 V_{NHE})
83 (Steele and Appelman, 1982). Because of its strong electrophilic character, PMS can
84 oxidise/degrade contaminants by electron-withdrawing with carbon nanotube as electron-
85 transfer mediator (Yun et al., 2017). It has been reported that PMS can rapidly inactivate the
86 disease-associated prion protein. In this process, the amino acid residues of prion protein
87 were oxidised by PMS through the formation of methionine sulfone and hydroxylated
88 tryptophan residues (Chesney et al., 2016). The transformation of methionine sulfoxide to
89 methionine sulfone might be explained by the oxygen transfer mechanism mentioned above.
90 However, the formation of hydroxylated tryptophan residues suggested that there might be
91 other reaction pathways for the PMS non-radical process, especially for nitrogenous
92 compounds.
93 In this study, the reactivity of PMS with various nitrogen-containing compounds was
94 investigated, including nitrogenous heterocyclic compounds, aliphatic amines, and
95 fluoroquinolones (Table 1). Degradation kinetics experiments (i.e., involving the effect of pH,
96 and common water matrix components) were conducted on the selected fluoroquinolones due
97 to their high reactivity with PMS. Fluoroquinolones are among the most consumed antibiotic
98 classes in the world. Due to their resistance to biodegradation and high adsorption affinity,
99 fluoroquinolones show long half-life times in the environment (e.g., 10.6 days in surface
100 water and 580 days in soil). Fluoroquinolones have been detected in wastewater, surface
101 water, groundwater and sediment/soil at concentrations ranging from ng/L to mg/L (Van

Doorslaer et al., 2014). As shown in Table 1, fluoroquinolones are characterized by a core quinolone ring structure containing a nitrogen atom. Ciprofloxacin, norfloxacin, and enrofloxacin also have a piperazine ring with two more amine nitrogen atoms. The transformation products of ciprofloxacin and enrofloxacin after PMS exposure were tentatively identified by high-resolution mass spectrometry. MS^2 and MS^3 fragmentation were applied for most compounds for structural identification. Based on the characteristics of the transformation products, possible reaction mechanisms of PMS reaction with nitrogenous compounds were proposed. Agar diffusion tests were applied to investigate the residual antibacterial activity of ciprofloxacin after PMS oxidation.

111 Table 1. Compounds investigated in this study

Adenine	Cytosine	Caffeine	Benzotriazole
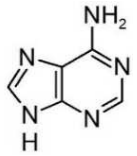	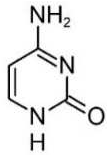	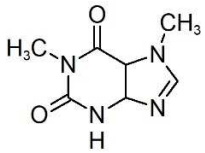	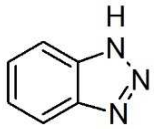
Metoprolol	Venlafaxine	Ciprofloxacin (CIP) pK_a=6.2, 8.8 [a]	Norfloxacin
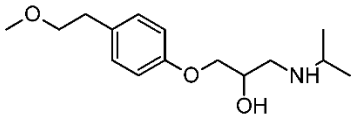	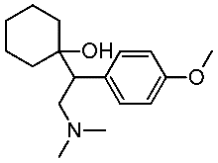	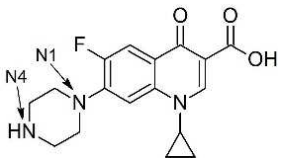	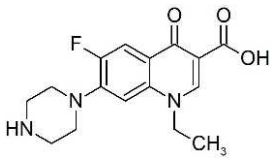
Enrofloxacin (ENR) pK_a=6.1, 7.7 [a]	Flumequine	1-(2-fluorophenyl) piperazine	
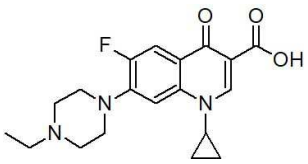	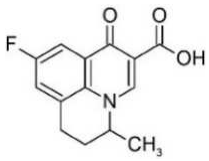		

[a] pK_a values were obtained from Jiang et al. (2016)

112

2. Materials and methods

2.1 Chemical Reagents

All chemicals were of analytical grade or higher and used as received without further purification. Potassium peroxymonosulfate (available as Oxone®), adenine (≥99%), cytosine (≥99%), caffeine (>99%), benzotriazole (99%), ciprofloxacin (≥98%), norfloxacin (≥98%), enrofloxacin (≥98%), flumequine (≥97%), 1-(2-fluorophenyl) piperazine (97%), metoprolol ((≥98.5%), venlafaxine (≥98%), *tert*-butanol (≥99%), and ethanol (pure) were purchased from Sigma-Aldrich. The Suwannee River hydrophobic acid fraction was previously isolated (Croué et al., 2000) and used to study the effect of natural organic matter (NOM) on the degradation rate of ciprofloxacin by PMS. All solutions were prepared in ultrapure water (18.2 MΩ cm, Milli-Q, Purelab Classic).

2.2 Experimental Procedures

Experiments were conducted in amber glass bottles at room temperature (22±1°C). Predetermined volumes of target compounds and PMS stock solutions were injected into 25 mL of 10 mM phosphate (pH = 6.2−8) or borate (pH = 8.2−11) buffer to obtain the desired initial concentrations. Samples were periodically collected and quenched with excess sodium thiosulfate. For most experiments, the initial concentrations used for target compound and PMS were 5 and 100 μM, respectively. To better identify the transformation products, high concentrations of ciprofloxacin and enrofloxacin (50 μM) were treated with 50 μM and 1 mM of PMS. The influence of dissolved oxygen on the formation of transformation products from enrofloxacin was investigated by purging the solution (before PMS spiking) with N_2 until the dissolved oxygen concentration was reduced to 0.21 mg/L. The solution was kept in N_2-purging throughout the experiment (20 min). The concentration of dissolved oxygen was measured using a WTW Oxi 330 Oxygen meter. For antibacterial

activity tests, 5 μM of ciprofloxacin was degraded by 100 and 250 μM PMS. Most experiments were conducted at least in duplicate.

2.3 Analytical Methods

A quantitative analysis of target compounds was conducted with a High-Performance Liquid Chromatography (HPLC, Agilent 1100) coupled with a Diode Array Detector (DAD, Agilent 1100) and an XDB-C18 column (5 μm, 4.6 × 150 mm, Agilent). Mobile phase composition followed various isocratic mixtures of methanol or acetonitrile with 10 mM phosphate buffer. All compounds were analysed at their maximum UV absorption. Detailed information on HPLC methods is provided in the supporting information section (Table S1). The concentration of the residual PMS was determined according to an ABTS colorimetric method previously published (Zhang et al., 2016). Briefly, 1 mL of sample was spiked into a mixed solution of 0.5 mL of ABTS (20 mM) and 0.2 mL of $CoSO_4$ (20 mM), then allowed to react for 1 min where a green-colored ABTS radical was formed. Then, 10 mL of H_2SO_4 (2%) was immediately added, followed by the spectrometric measurement at 734 nm (Cary 60, Agilent). The transformation products of ciprofloxacin and enrofloxacin were identified using an Accela 600 Liquid Chromatography system coupled to a High-Resolution Mass Spectrometry (LC-HRMS, LTQ Orbitrap XL, Thermo Fisher), and fitted with an Electrospray Ion Source (ESI). Compounds were separated on a kinetex C18 column (2.6 μm, 100×2.1 mm, Phenomenex). Full scan and MS^2 fragmentation scans were acquired in positive ionisation mode (+eV). MS^3 fragmentation was additionally applied for compounds with major peak areas on LC-HRMS. Details on LC-HRMS parameters are provided in Table S2.

The distribution coefficients (log*D*) of compounds were calculated on a public Web source developed by ChemAxon (https://chemicalize.com, accessed in July 2019).

2.4 Antibacterial Activity Test

Agar disk-diffusion tests were conducted to investigate the antibacterial activity of ciprofloxacin (5 μM) after PMS exposure (100 and 250 μM) using *Escherichia. coli* B (*E. coli* B) as the test microorganism according to the Clinical and Laboratory Standards Institute (CLSI, 2012). Briefly, lysogeny (LB) agar plates were inoculated with 100 μL of an overnight culture of *E. coli* B, equivalent to 0.5 McFarland. Then, blank antibiotic cartridges (approximately 6 mm in diameter) containing the test solutions, were placed on the agar surface. The diameters of inhibition zones around discs were measured after the plate was incubated overnight at 37°C. A wider zone of no growth indicates a stronger antibacterial activity of the test solution. The removal of ciprofloxacin antibacterial activity after PMS exposure was determined by comparing the diameters of the inhibition zones from PMS-treated samples of ciprofloxacin and the ciprofloxacin standards with known concentrations (0.2, 0.5, 1, 2, 3, 4, and 5 μM). Each sample was tested in triplicates.

3. Results and Discussion

3.1 Reactivity of PMS with various nitrogen containing compounds

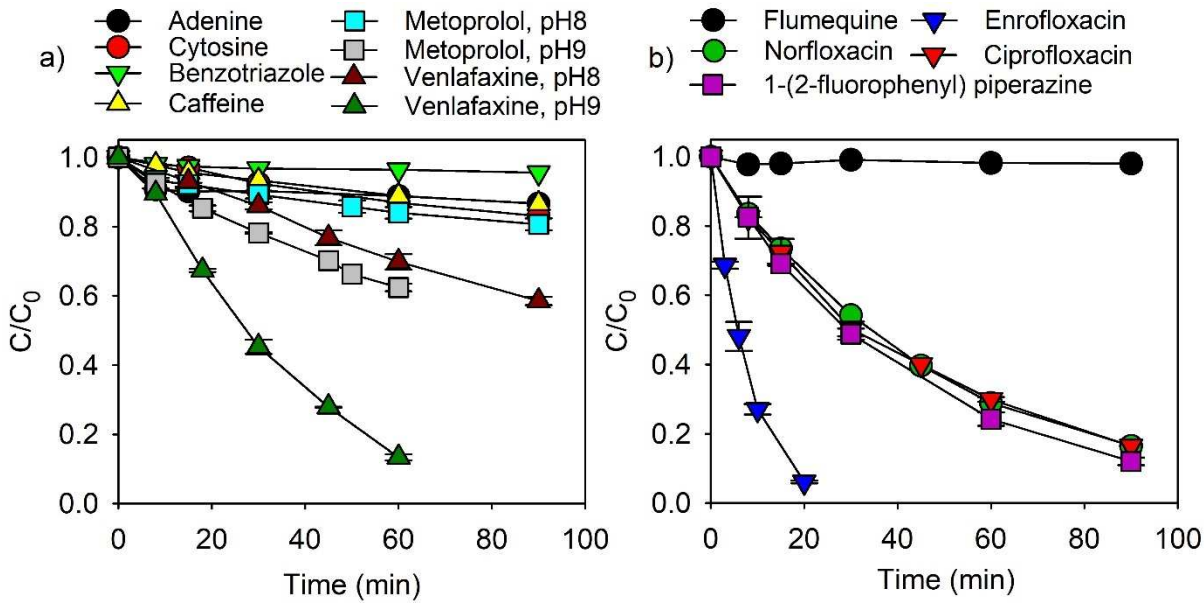

Figure 1. Relative removal of the selected nitrogenous compounds by PMS (Target compound: 5 μM; PMS: 100 μM; 10 mM phosphate buffer at pH 8; Metoprolol and venlafaxine were also tested in 10 mM borate buffer at pH 9)

The degradation of the selected nitrogenous compounds by PMS was individually studied in the absence of chemical catalysts or UV irradiation. Less than 20% of the selected nitrogenous heterocyclic compounds (i.e., adenine, cytosine, benzotriazole, and caffeine) were removed at pH 8 within 90 min (Figure 1a). Approximately 40% of venlafaxine (aliphatic tertiary amine) was eliminated at pH 8 for the same time frame, which was faster than metoprolol (aliphatic secondary amine). The degradation of metoprolol and venlafaxine by PMS was influenced by pH, suggesting that the amine group was likely the main reaction site. The degradation rates were faster at pH 9 than at pH 8 for both compounds, possibly due to the higher proportion of deprotonated molecules at higher pH. Venlafaxine was degraded

faster than metoprolol in both conditions, revealing that PMS might be more reactive with tertiary amines than secondary amines.

The degradation efficiencies of fluoroquinolones and their related compounds significantly varied depending on their structural characteristics (Figure 1b). Flumequine, a fluoroquinolone without a piperazine ring (Table 1), was stable in the presence of PMS in these experimental conditions, suggesting that PMS does not react with quinolone rings. The cyclopropane ring of ciprofloxacin (CIP) is substituted by an ethyl group in norfloxacin. 1-(2-fluorophenyl) piperazine has a fluorobenzene ring instead of the quinolone ring. However, CIP, norfloxacin, and 1-(2-fluorophenyl) piperazine have the same piperazine ring structure and exhibited comparable degradation rates toward PMS (80% removal within 90 min). These results indicated that the piperazine ring was the main reaction site for PMS. This was further supported by LC-HRMS analyses (section 3.4) from which only piperazine ring cleavage products were identified after PMS exposure. The N4 (CIP in Table 1 for atom numbering) in the piperazine ring of enrofloxacin (ENR) is substituted by an ethyl group (tertiary amine), which differs from CIP (secondary amine). ENR was degraded considerably faster than CIP, a result that was consistent with the above evidence that tertiary amines were more susceptible to PMS attack than secondary amines. Overall results suggested that PMS was more reactive towards fluoroquinolones (except for flumequine) than the selected nitrogenous heterocyclic compounds and aliphatic amines at pH 8. More detailed experiments were conducted on CIP and ENR to study the reaction mechanism of PMS with nitrogenous compounds.

3.2 Degradation kinetics of fluoroquinolones by PMS

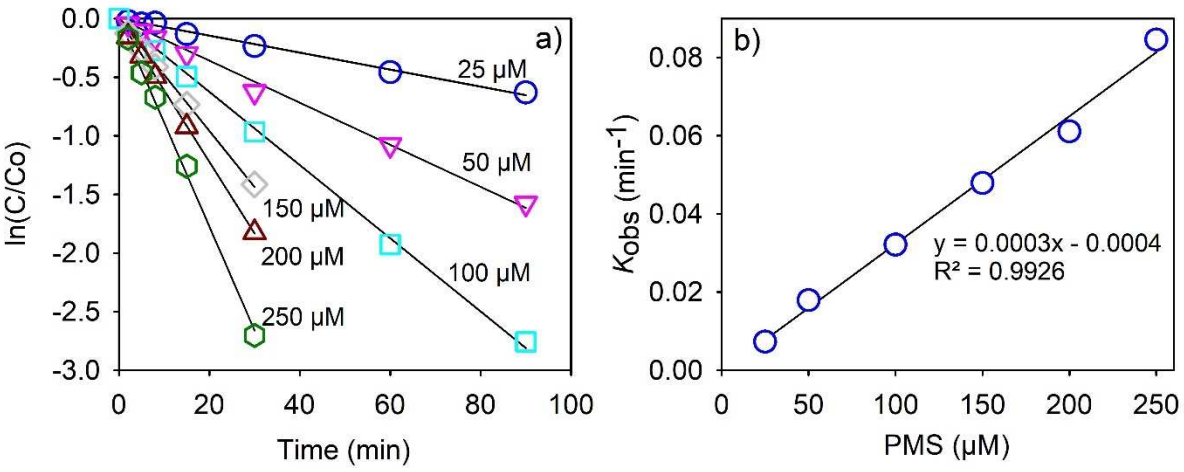

211

212 **Figure 2.** a) Effect of the initial concentration of PMS on ciprofloxacin degradation; b) k_{obs}

213 versus initial concentration of PMS (Ciprofloxacin: 5 μM; 10 mM borate buffer at pH 8.2)

214 The presence of excess ethanol, *t*-BuOH, and NaN_3 did not affect the degradation kinetic of

215 CIP (Figure S1), which confirmed previous findings that no $SO_4^{\bullet-}$, $^{\bullet}OH$, and $^1O_2$ were

216 involved during the oxidation of fluoroquinolones by PMS (Zhou et al., 2018). The

217 degradation of CIP was promoted by increasing the initial PMS dose (25–250 μM), following

218 pseudo-first order kinetics (R^2>0.99) (Figure 2a). The measured rate constants, k_{obs}, were

219 derived from the slope of $\ln(C/C_0)$ versus time. As shown in Figure 2b, k_{obs} exhibited a

220 linear relationship toward the initial PMS dose, suggesting that the overall reaction rate can

221 be described by the second-order kinetic. According to equation 1 and 2, the apparent second-

222 order rate constant, k_{app}, of CIP with PMS was calculated as 5.28 ± 0.08 (M^{-1} s^{-1}) at pH 8.2,

223 which was comparable with previously reported results by Zhou et al. (2018) (~ 6 M^{-1} s^{-1} at

224 pH 8).

225 $$\frac{d[CIP]}{dt} = -k_{obs}[CIP] \qquad (1)$$

226 $$\frac{d[CIP]}{dt} = -k_{app}[CIP][PMS] \qquad (2)$$

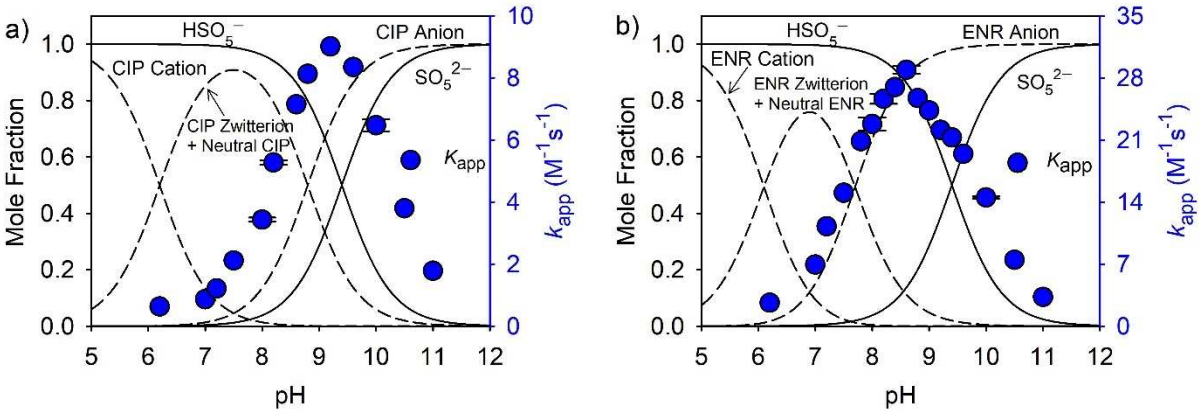

227

228 **Figure 3.** The effect of pH on the distribution of acid-base species of ciprofloxacin (a) and
229 enrofloxacin (b), and their apparent second-order constants with PMS. (CIP or ENR: 5 μM;
230 PMS: 100 μM; 10 mM phosphate or borate buffer at pH 6.2−11; The acid-base species of
231 ciprofloxacin were shown in Scheme S1 as an example)

232 As illustrated in Figure 3, the degradation efficiency (k_{app}) of CIP and ENR by PMS were
233 highly pH-dependent. The pH-dependent reactivity of fluoroquinolones was also observed
234 with free chlorine (Dodd et al., 2005), manganese oxide (Zhang and Huang, 2005), ozone
235 (Dodd et al., 2006), and chlorine dioxide (Wang et al., 2010). The pH-dependence of
236 fluoroquinolones degradation can be explained by the change in the distribution of
237 fluoroquinolones and PMS acid-base species with pH (Zhou et al., 2018). The pK_a values of
238 CIP and ENR relevant to these experimental conditions were provided in Table 1. pK_{a1} and
239 pK_{a2} were related to the deprotonation of the carboxylic group and the protonation of N4 in
240 the piperazine ring, respectively (Scheme S1) (Takács-Novák et al., 1990). PMS dissociated
241 into SO_5^{2-} at alkaline pH ($HSO_5^- + H_2O \rightleftarrows SO_5^{2-} + H_3O^+$, p$K_{a2}$=9.4) (Ball and Edwards,
242 1956). The k_{app} values of CIP and ENR increased with increasing molar fraction of the
243 anionic species (Figure 3), suggesting that the anion forms of CIP and ENR were most
244 susceptible to PMS oxidation. In general, N4 in piperazine ring is deprotonated when CIP and
245 ENR are present in anionic form, consequently showing a stronger nucleophilic character.

The highest k_{app} values of CIP and ENR were found at around pH 9 and pH 8.6, respectively; then, it sharply decreased with increasing relative abundance of SO_5^{2-}, suggesting that SO_5^{2-} is a weaker oxidant compared to PMS. SO_5^{2-} was also reported as less reactive than PMS with β-lactam antibiotics, due to its weaker electrophilic property (Chen et al., 2018). Notably, PMS showed higher reactivity towards ENR than CIP in all studied pH conditions.

3.3 Comparison with other peroxides and the effect of the water matrix

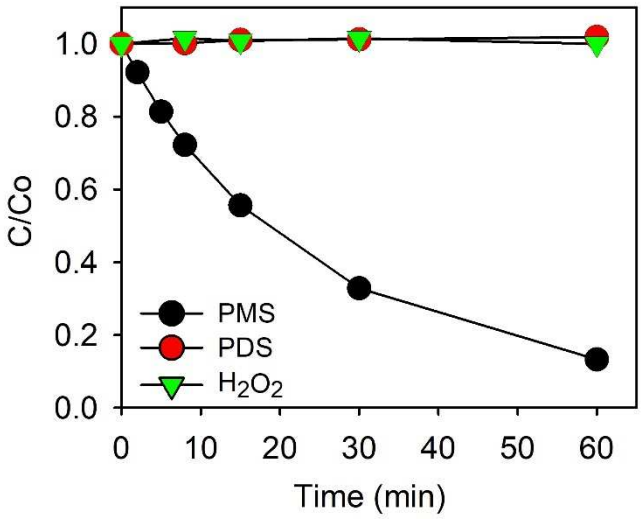

Figure 4. Relative removal of ciprofloxacin by PMS, PDS, and H_2O_2 (Ciprofloxacin=5 μM; Oxidants=100 μM; 10 mM phosphate buffer at pH 8)

The reactivity of PMS was compared with other peroxides. Unlike PMS, PDS and H_2O_2 did not react with CIP under the same experimental conditions (Figure 4). These results suggested that PDS and H_2O_2, as symmetric peroxides, tend to be more stable; whereas, PMS is a more efficient electron acceptor, possibly due to its asymmetric structure (Lei et al., 2016). This is consistent with previous findings indicating that PMS was more efficient compared to PDS for the removal of organic contaminants during the mediated electron transfer through carbon nanotubes (Yun et al., 2017; Yun et al., 2018).

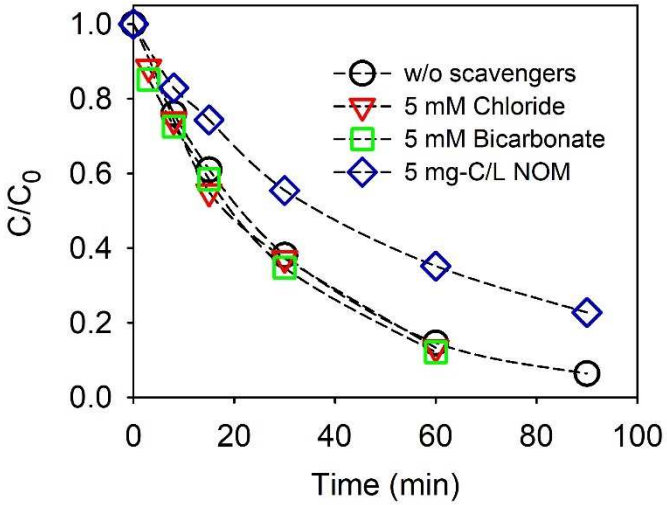

262

263 **Figure 5.** Effect of the water matrix on the degradation of ciprofloxacin by PMS
264 (Ciprofloxacin: 5 μM; PMS: 100 μM; Chloride= Bicarbonate: 5 mM; NOM: 5 mg-C/L; 10
265 mM borate buffer at pH 8.2)

266 The water matrix components can compete with the target contaminants to consume radicals
267 during AOPs, consequently lowering the treatment efficiency. The effect of the common
268 water matrix components (i.e., NOM, chloride, and bicarbonate ions) on the degradation of
269 CIP by PMS was investigated. Unlike the radical-based AOPs, the degradation of CIP by
270 PMS was not impacted by the presence of 5 mM of chloride and bicarbonate ions (Figure 5).
271 PMS was previously reported to oxidize chloride ion into chlorine, which can contribute to
272 contaminant degradation (Fortnum et al., 1960). However, the acceleration of the CIP
273 degradation rate was not observed in this study upon the addition of 5 mM of chloride. This
274 can be explained by the insufficient formation of chlorine due to the low reaction rate
275 constant of chloride with PMS (1.4×10^{-3} M^{-1} s^{-1}) (Fortnum et al., 1960), which was about
276 three orders of magnetic lower than the k_{app} of CIP with PMS in this study (5.28 ± 0.08 M^{-1}
277 s^{-1} at pH 8.2). The addition of 5 mg-C/L NOM slightly inhibited the removal of CIP,
278 suggesting that PMS can react with NOM.

3.4 Transformation products

Table 2. Transformation products of ciprofloxacin (CIP) detected by LC-HRMS

Compound	RT[a]	Molecular formula	Molecular mass[b]	MS^{2} [c], *m/z*	Proposed structures
CIP	12.6	$C_{17}H_{19}O_3N_3F$	332.1404 (-0.169)	314, 288	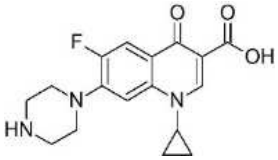
P263	16.7	$C_{13}H_{12}O_3N_2F$	263.0826 (-0.369)	245, 263	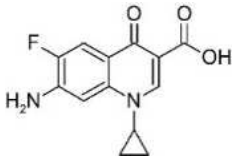
P291	17.4	$C_{14}H_{12}O_4N_2F$	291.0775 (-0.177)	273, 291	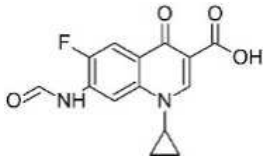
P306	12.3	$C_{15}H_{17}O_3N_3F$	306.1248 (-0.183)	306, 288	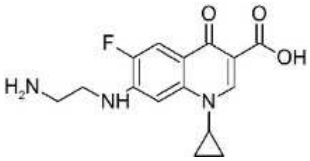
P320	18.0	$C_{15}H_{15}O_4N_3F$	320.1034 (-0.252)	302, 320 MS^{3}: 258, 265, 285, 302, 224, 245, 217	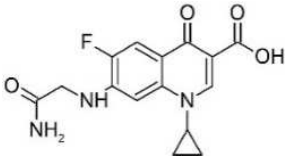
P334a	11.1	$C_{16}H_{17}O_4N_3F$	334.1198 (-0.750)	316, 317, 314, 306, 296 MS^{3}: 296, 245,	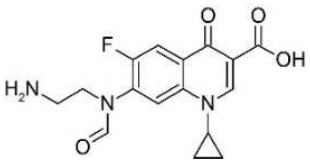

				230, 271, 288	
P334b	17.3	$C_{16}H_{17}O_4N_3F$	334.1199 (-0.301)	316 MS^3: 271, 289, 298, 245	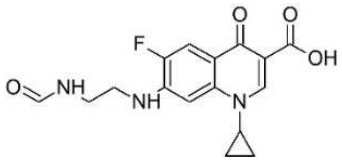
P348a	8.2	$C_{17}H_{19}O_4N_3F$	348.1348 (-1.841)	331, 287, 304 MS^3: 287, 273	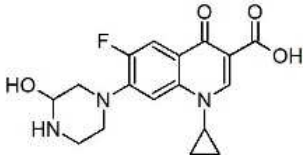
P348b	17.3	$C_{17}H_{19}O_4N_3F$	348.1354 (-0.002)	330, 287 MS^3:285, 272, 310, 282	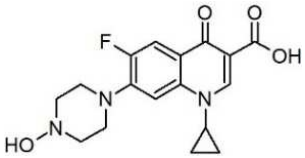
P362	13.2	$C_{17}H_{17}O_5N_3F$	362.1143 (-0.985)	344, 362	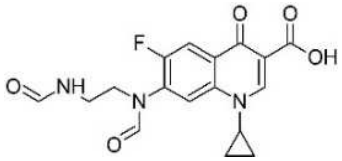
P364a	12.4	$C_{17}H_{19}O_5N_3F$	364.1302 (-0.372)	346, 364 MS^3: 326, 288, 271	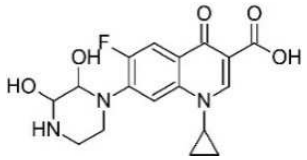
P364b	16.5	$C_{17}H_{19}O_5N_3F$	364.1239 (-0.372)	346, 364, 328 MS^3: 346, 328, 275, 257	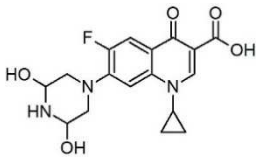

[a] Retention time (min); [b] Experimental mass for $[M+H]^+$; numbers in brackets represent the difference with the theoretical mass of the proposed compound (ppm); [c] MS^3 fragmentation was additionally applied for P320, P334 (a, b), P348 (a, b) and P364 (a, b). The MS^2/MS^3 spectra of compounds were provided in the supporting

information (Figure S2-S13).

Eleven transformation products of CIP after PMS oxidation were detected by LC-HRMS (Table 2). Their structures were tentatively proposed based on the accurate mass derived from HRMS and MS^2/MS^3 fragmentation patterns (Figure S2-S13). The proposed structures indicated that the degradation of CIP occurred by the hydroxylation and dealkylation of the piperazine ring, with the subsequent formation of aldehyde and amide moieties. The core quinolone ring of CIP remained intact and no defluorination or decarboxylation products were detected, which were the known transformation products of CIP during Fenton oxidation (Giri and Golder, 2014), $SO_4^{\bullet-}$ (Jiang et al., 2016) and photolytic reactions (Paul et al., 2010). These results were consistent with the fact that flumequine, which does not incorporate a piperazine ring, did not react with PMS (Figure 1b). Several transformation products (e.g., P263, P291, P306, P334, P348, P362, and P364) were also obtained during the oxidative transformation of CIP by manganese oxide (Zhang and Huang, 2005), chlorine dioxide (Wang et al., 2010), permanganate (Hu et al., 2011), and Ferrate (VI) (Yang et al., 2016a), revealing that PMS may share a similar reaction mechanism with these oxidants. However, structural isomers corresponding to CIP with one additional oxygen atom (P348a and P348b) or two additional oxygen atoms (P364a and P364b) were detected in this study. Particularly, P348a and P348b shared the same molecular weight, but different MS^2/MS^3 spectra (Figure S9 and S10, respectively) and retention time. P348a was proposed as a hydroxylated analogue of CIP, with a hydroxyl group located on α-carbon; whereas, P348b was a hydroxylamine compound. This may be further supported by the calculated distribution coefficient (log*D*) at pH 2.3 (pH of LC-HRMS mobile phase). P348b had a higher log*D* (1.15) than P348a (-2.05), consequently showing a longer retention time on the reverse phase column. P348b was believed to be rearranged from its *N*-oxide analogue, which is a known mechanism for primary and secondary amines (Hübner et al., 2015). Most transformation

products (except for P263, P306, and P348) were not reported in a previous study on the oxidation of 20 μM CIP by 0.1 mM PMS (Zhou et al., 2018), likely because higher CIP (50 μM) was applied in the current study to maximize the formation of by-products. Moreover, the HRMS signal intensity of most products (e.g., P320, P334, P291) reached their maximum when the PMS exposure was above 8 (mM × min) (Figure 6), which was achieved by initially applying 1 mM PMS in this study.

To the best of our knowledge, the transformation product P320 has only been reported from the ozonation of CIP (Liu et al., 2012). The MS^3 spectrum (Figure S6b) of P320 exhibited a dominant ion cluster *m/z* 258 corresponding to the loss of an amide group ($-CH_2ON$) from the major ion cluster *m/z* 302 in its MS^2 spectrum (Figure S6a). Thus, the postulated structure of P320 is an amide moiety formed at the secondary aliphatic amine (N4) of the piperazine ring.

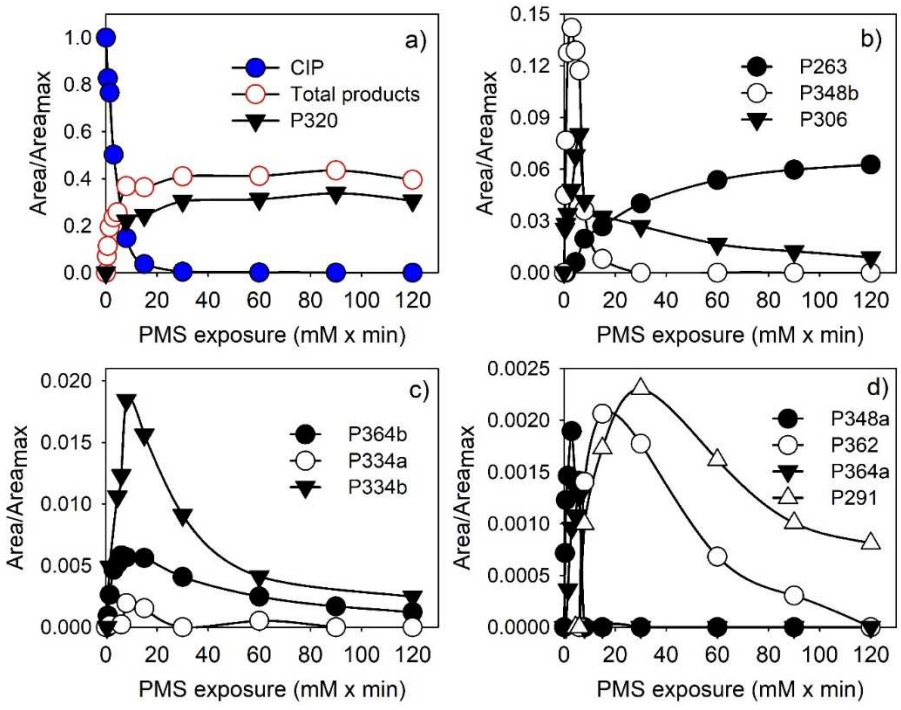

Figure 6. The evolution of the normalized chromatographic peak areas of ciprofloxacin (CIP) and its transformation products with PMS exposure. $Area_{max}$ represents the peak area of

ciprofloxacin at t=0 (Ciprofloxacin: 50 μM; PMS: 0.05 and 1 mM; 10 mM borate buffer at pH 8.2)

Figure 6 presents the evolution of the normalized chromatographic peak areas of CIP and its transformation products with PMS exposure. P320 exerted the largest peak area among all identified transformation products (i.e., close to the sum of the peak areas of all transformation products). P320 was rapidly formed with the degradation of CIP and reached a plateau. P263, which refers to the complete loss of the piperazine ring, gradually increased with exposure time. Thus, P320 and P263 were the final products in these experimental conditions, while all other compounds were intermediates showing a maximum production at different oxidant exposures. For example, P334b and P362 reached their highest peak areas at 8 and 15 (mM × min), respectively, while P320 almost reached a plateau, indicating that P334b and P362 were unlikely the intermediates of P320.

Hydroxylated products (P376 and P392) were the major by-products after PMS oxidation of ENR (Table S3), which was in accordance with a previous study (Zhou et al., 2018). Like CIP, two structural isomers of ENR with an additional oxygen atom (i.e., P376a and P376b) were identified. P376a was proposed as a hydroxylated ENR on α-carbon, while P376b was a *N*-oxide analogue of ENR, although further confirmation with analytical standards is needed. The log*D* value of P376b at pH 2.3 (1.09) was considerably higher than ENR (-1.19) and P376a (-1.65), consistent with its longer retention time on the LC-HRMS chromatogram (Table S3). Previous investigations have demonstrated that *N*-oxide analogues of tertiary amines have higher retention times than their precursors on reverse-phase columns (Merel et al., 2017). A transformation product of ENR after PMS oxidation was detected on the HPLC-UV chromatogram (Figure S14), which was eluted after the ENR peak and proposed as P376b based on an assumption that the eluting order of compounds was comparable on LC-HRMS and HPLC-UV coupled with similar reverse-phase C18 columns. The HPLC-UV

peak area of P376b did not change during the experiments conducted with and without N_2-purged solutions (Figure S15). These results suggested that the dissolved oxygen did not contribute to the formation of ENR *N*-oxide. Alternatively, the oxygen likely originated from PMS itself. The *N*-oxide formation was also proposed for ENR oxidized by ozone (Dodd et al., 2006), manganese oxide (Zhang and Huang, 2005), and permanganate (Xu et al., 2016).

3.5 Proposed reaction mechanisms

Scheme 1. Proposed degradation mechanisms of ciprofloxacin (a) and enrofloxacin (b) by PMS (Ia, Ib, and Ic are the proposed intermediates)

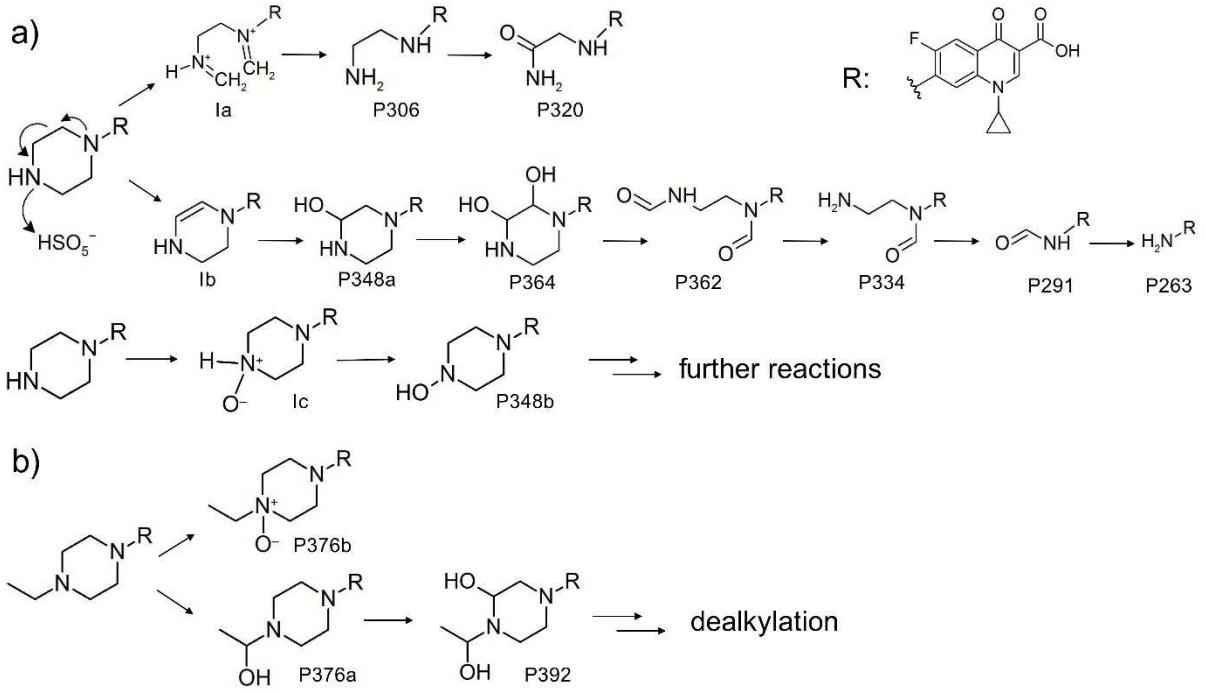

In accordance with the postulated structures of the transformation products and the evolution of their peak areas on LC-HRMS chromatograms, reaction mechanisms for the oxidative transformation of CIP by PMS were proposed (Scheme 1a). The reaction was initiated by the direct electron transfer from the piperazine ring to PMS. In this process, PMS acted as an electron acceptor, rather than a radical precursor, to directly oxidize CIP. The N4 atom of piperazine ring was the critical site for the electrophilic attack of PMS. The N1 atom is

known as less reactive to electrophiles than N4 due to its direct connection to the fluoroquinolone ring substituted by strong electron-withdrawing fluorine and –COOH (Dodd et al., 2005; Giri and Golder, 2014). Nevertheless, previous studies have demonstrated that the piperazine ring should be considered as a whole reaction centre with the contribution of both nitrogen atoms to electron-transfer (Wang et al., 2010). This could explain the higher reactivity of PMS with piperazine ring-containing compounds, compared to aliphatic amines (metoprolol and venlafaxine), as shown in Figure 1.

The initial electron transfer from the piperazine ring to PMS produces an imine intermediate (Ia, Scheme 1a) as proposed by Dodd et al. (2005) and Wang et al. (2010) for the oxidation of CIP by free chlorine and chlorine dioxide, respectively. The hydrolysis of the imine intermediate rapidly induced the dealkylation of the piperazine ring to generate P306. The subsequent electron transfer from the amine group of P306 to PMS was followed by hydrolysis producing P320. The presence of highly electron-withdrawing carbonyl group (C=O) in P320 possibly limited the electron transfer from amide-N to PMS. Thus, P320 was stable in the presence of excess PMS (Figure 6a). The formation of hydroxylated products P348a and P364 suggested the presence of a similar enamine intermediate (Ib, Scheme 1a), which has been proposed for the reactions of permanganate (Hu et al., 2011) and Ferrate (IV) (Yang et al., 2016a) with CIP. The double bond of enamine can be oxidized to aldehyde moieties (P362, P334, and P291), leading to the complete degradation of piperazine ring.

The oxygen transfer from PMS to secondary amine CIP generates *N*-oxide intermediate (Ic, Scheme 1a), which subsequently rearranged to hydroxylamine compound (P348b) (Lee and von Gunten, 2016). As shown in Figure 6b, the intensity of P348b reached the maximum at 3 mM (mM × min) and rapidly decreased with PMS exposure, suggesting that P348b was subjected to further reactions in the presence of excess PMS. The oxygen transfer pathway might involve the transfer of the distal oxygen in the peroxide bond of PMS to CIP. An

oxygen transfer mechanism was also proposed for the oxidation of arsenite As (III) to As (V) by PMS (Wang et al., 2014). The thioether sulfur of β-lactam antibiotics can be substituted by the oxygen from PMS to produce sulfoxide products (Chen et al., 2018). The aniline moieties of sulfonamide antibiotics can be converted to nitroso or nitrobenzene moieties through PMS oxygen substitution (Yin et al., 2018).

PMS was also proposed to react with tertiary amine ENR via oxygen transfer to generate ENR *N*-oxide, P376b (Scheme 1b). The direct electron transfer pathway also occurred during PMS oxidation of ENR and led to the hydroxylation on α-carbon to produce P376a and P392. Based on the degradation pathway of CIP, it was postulated that the hydroxylated products P392 might undergo further oxidation, followed by the dealkylation of the piperazine ring.

Additional investigation is needed to confirm the major pathway of PMS reaction (electron transfer *vs* oxygen transfer) with nitrogenous compounds, which might be helpful to explain the different reaction potential of PMS towards secondary and tertiary amine moieties as mentioned above.

3.6 Antibacterial activity assays

Fluoroquinolones inhibit the bacterial DNA replication by hydrogen binding and charge interactions with the relaxed DNA. The core quinolone structure would be responsible for DNA-binding (Dodd et al., 2006), while the fluorine substitute plays an important role in inhibiting the DNA gyrase and enhancing cell permeation (Serna-Galvis et al., 2017).

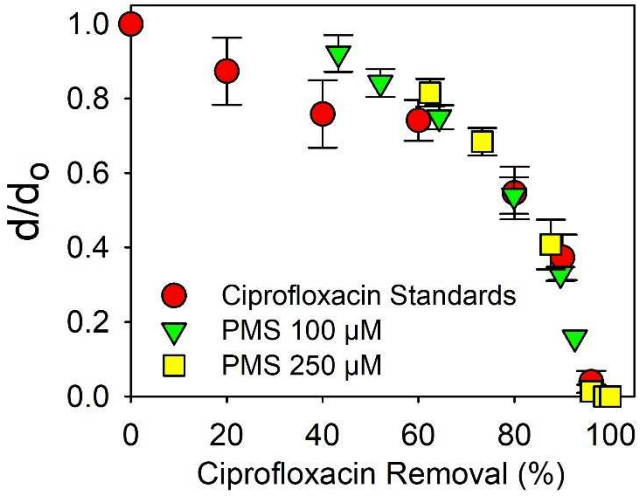

404

405 **Figure 7.** Antibacterial activity removal of ciprofloxacin (CIP) during PMS treatment. d_0
406 represents the diameter of the inhibition zone in agar plate formed by 5 µM of CIP standard
407 solution (CIP standards: 0.2, 0.5, 1, 2, 3, 4 and 5 µM; for PMS treatment, initial concentration
408 of CIP:5 µM, PMS: 100 and 250 µM, 10 mM borate buffer at pH 8.2)

409 Based on LC-HRMS results, the transformation products of CIP after PMS treatment still
410 retained the core quinolone structure, raising concerns about the residual antibacterial activity.
411 Thus, agar diffusion assays were conducted with *E. coli B* as an indicator. As shown in
412 Figure 7, the antibacterial activity of the solution gradually reduced with the removal of CIP
413 during PMS treatment. However, after 40 to 50% removal of CIP with 100 µM of PMS, the
414 sample resulted in a larger inhibition zone in the agar plate than CIP standard solutions. This
415 result indicated that the transformation products at an earlier stage (e.g., hydroxylamine
416 product P348b, Figure 6b) might still exert antibacterial potency. The residual antibacterial
417 activity was efficiently removed with the complete degradation of CIP, suggesting that the
418 major final products P320 and P263 showed negligible antibacterial activity compared to CIP.
419 The structural modifications on the piperazine ring alter the acid-base speciation and
420 significantly affect fluoroquinolones cell permeation (Paul et al., 2010). Although the amide
421 and aldehyde moieties produced after PMS exposure kept the core quinolone structure in this

study, their physicochemical characteristics might be significantly different from those of CIP, consequently reducing their uptake by bacteria cell and binding to DNA. The current results were in agreement with previous findings reporting that the photolytic transformation products of CIP retaining the quinolone ring significantly diminished the antibacterial potency of the parent antibiotic (Paul et al., 2010).

4. Conclusion

- PMS can efficiently degrade the selected fluoroquinolones (except for flumequine), followed by aliphatic amines and nitrogenous heterocyclic compounds. The common water matrix components (e.g., bicarbonate and chloride ions) did not impact the degradation rate of CIP by PMS. The electron transfer from the piperazine ring of CIP to PMS induced the dealkylation and hydroxylation of the molecule and led to the formation of amide and aldehyde moieties. PMS was also proposed to react with CIP and ENR via oxygen transfer to produce hydroxylamine analogue of CIP and ENR *N*-oxide, respectively.
- PMS efficiently removed the antibacterial activity of CIP. However, the transformation products in earlier stages of the reaction still exerted antibacterial potency. A complete elimination of the parent compound, as well as its transformation products, is required during the fluoroquinolone treatment by PMS.

The findings of this study suggested that the direct PMS oxidation can be selectively applied for the removal of nitrogenous compounds (e.g., fluoroquinolones). However, some persistent transformation products (e.g., *N*-oxides) can be formed, which are inert to the biodegradation (Hübner et al., 2015). Unlike radical-based processes, this treatment can maintain its efficiency in complex water matrixes. However, NOM slightly inhibited the degradation of CIP by PMS. Therefore, additional studies are needed to investigate the

reactivity of PMS with NOM fractions of different characteristics to optimize the PMS dose for its best treatment efficiency. Because environmental components (e.g., nitrogen and sulfur-containing organics) (Chen et al., 2018; Yang et al., 2018) are susceptible to react with PMS, the non-radical pathway might hinder the formation of radicals during PMS-activated AOPs, consequently limiting the removal of the targeted hazardous compounds. The electron and oxygen transfer pathways proposed in this study assist in understanding the non-radical reaction mechanism of PMS with organic contaminants and in predicting the formation of potential transformation products. Similar mechanistic studies and screening of transformation products can be extended to other oxidants used during water treatment, which also have similar peroxide bond and asymmetric structure to PMS, such as organic peracids (Luukkonen and Pehkonen, 2017).

Acknowledgments

Curtin University (Curtin International Postgraduate Research Scholarship) and Water Research Australia (WaterRA Postgraduate Scholarship) are gratefully acknowledged for providing financial support for M. Nihemaiti. The authors would like to thank Dr Francesco Busetti and Dr Zuo Tong How for their support on LC-MS analysis, and Dr Leonardo Gutierrez (Universidad del Pacifico) for proofreading.

References

Ball, D.L.Edwards, J.O., 1956. The Kinetics and Mechanism of the Decomposition of Caro's Acid. I. Journal of the American Chemical Society 78(6), 1125-1129.

Chen, J., Fang, C., Xia, W., Huang, T.Huang, C.-H., 2018. Selective Transformation of β-Lactam Antibiotics by Peroxymonosulfate: Reaction Kinetics and Nonradical Mechanism. Environmental Science & Technology 52(3), 1461-1470.

Chesney, A.R., Booth, C.J., Lietz, C.B., Li, L.Pedersen, J.A., 2016. Peroxymonosulfate Rapidly Inactivates the Disease-Associated Prion Protein. Environmental Science & Technology 50(13), 7095-7105.

CLSI, 2012. Performance Standards for Antimicrobial Disk Susceptibility Tests. Approved Standard, 7th ed. Clinical and Laboratory Standards Institute, Wayne, Pennsylvania, USA.

Croué, J.-P., Korshin, G.V.Benjamin, M., 2000. Characterisation of Natural Organic Matter in Drinking Water. American Water Works Association Research Foundation, Denver, CO, USA.

Dodd, M.C., Buffle, M.-O.von Gunten, U., 2006. Oxidation of Antibacterial Molecules by Aqueous Ozone: Moiety-Specific Reaction Kinetics and Application to Ozone-Based Wastewater Treatment. Environmental Science & Technology 40(6), 1969-1977.

Dodd, M.C., Shah, A.D., von Gunten, U.Huang, C.-H., 2005. Interactions of Fluoroquinolone Antibacterial Agents with Aqueous Chlorine: Reaction Kinetics, Mechanisms, and Transformation Pathways. Environmental Science & Technology 39(18), 7065-7076.

Fortnum, D.H., Battaglia, C.J., Cohen, S.R.Edwards, J.O., 1960. The Kinetics of the Oxidation of Halide Ions by Monosubstituted Peroxides. Journal of the American Chemical Society 82(4), 778-782.

Ghanbari, F.Moradi, M., 2017. Application of peroxymonosulfate and its activation methods for degradation of environmental organic pollutants: Review. Chemical Engineering Journal 310, 41-62.

Giri, A.S.Golder, A.K., 2014. Ciprofloxacin degradation from aqueous solution by Fenton oxidation: reaction kinetics and degradation mechanisms. RSC Advances 4(13), 6738-6745.

Hu, L., Stemig, A.M., Wammer, K.H.Strathmann, T.J., 2011. Oxidation of Antibiotics during Water Treatment with Potassium Permanganate: Reaction Pathways and Deactivation. Environmental Science & Technology 45(8), 3635-3642.

Hübner, U., von Gunten, U.Jekel, M., 2015. Evaluation of the persistence of transformation products from ozonation of trace organic compounds – A critical review. Water Research 68, 150-170.

Ike, I.A., Linden, K.G., Orbell, J.D.Duke, M., 2018. Critical review of the science and sustainability of persulphate advanced oxidation processes. Chemical Engineering Journal 338, 651-669.

Jiang, C., Ji, Y., Shi, Y., Chen, J.Cai, T., 2016. Sulfate radical-based oxidation of fluoroquinolone antibiotics: Kinetics, mechanisms and effects of natural water matrices. Water Research 106, 507-517.

Lee, Y.von Gunten, U., 2016. Advances in predicting organic contaminant abatement during ozonation of municipal wastewater effluent: reaction kinetics, transformation products, and changes of biological effects. Environmental Science: Water Research & Technology 2(3), 421-442.

509 Lei, Y., Chen, C.-S., Ai, J., Lin, H., Huang, Y.-H.Zhang, H., 2016. Selective decolorization
510 of cationic dyes by peroxymonosulfate: non-radical mechanism and effect of chloride.
511 RSC Advances 6(2), 866-871.
512 Liu, C., Nanaboina, V., Korshin, G.V.Jiang, W., 2012. Spectroscopic study of degradation
513 products of ciprofloxacin, norfloxacin and lomefloxacin formed in ozonated
514 wastewater. Water Research 46(16), 5235-5246.
515 Lutze, H.V., Bircher, S., Rapp, I., Kerlin, N., Bakkour, R., Geisler, M., von Sonntag,
516 C.Schmidt, T.C., 2015. Degradation of Chlorotriazine Pesticides by Sulfate Radicals
517 and the Influence of Organic Matter. Environmental Science & Technology 49(3),
518 1673-1680.
519 Luukkonen, T.Pehkonen, S.O., 2017. Peracids in water treatment: A critical review. Critical
520 Reviews in Environmental Science and Technology 47(1), 1-39.
521 Merel, S., Lege, S., Yanez Heras, J.E.Zwiener, C., 2017. Assessment of N-Oxide Formation
522 during Wastewater Ozonation. Environmental Science & Technology 51(1), 410-417.
523 Neta, P., Huie, R.E.Ross, A.B., 1988. Rate Constants for Reactions of Inorganic Radicals in
524 Aqueous Solution. Journal of Physical and Chemical Reference Data 17(3), 1027-
525 1284.
526 Paul, T., Dodd, M.C.Strathmann, T.J., 2010. Photolytic and photocatalytic decomposition of
527 aqueous ciprofloxacin: Transformation products and residual antibacterial activity.
528 Water Research 44(10), 3121-3132.
529 Serna-Galvis, E.A., Ferraro, F., Silva-Agredo, J.Torres-Palma, R.A., 2017. Degradation of
530 highly consumed fluoroquinolones, penicillins and cephalosporins in distilled water
531 and simulated hospital wastewater by UV254 and UV254/persulfate processes. Water
532 Research 122, 128-138.
533 Steele, W.V.Appelman, E.H., 1982. The standard enthalpy of formation of
534 peroxymonosulfate (HSO5−) and the standard electrode potential of the
535 peroxymonosulfate-bisulfate couple. The Journal of Chemical Thermodynamics 14(4),
536 337-344.
537 Takács-Novák, K., Noszál, B., Hermecz, I., Keresztúri, G., Podányi, B.Szasz, G., 1990.
538 Protonation Equilibria of Quinolone Antibacterials. Journal of Pharmaceutical
539 Sciences 79(11), 1023-1028.
540 Van Doorslaer, X., Dewulf, J., Van Langenhove, H.Demeestere, K., 2014. Fluoroquinolone
541 antibiotics: An emerging class of environmental micropollutants. Science of the Total
542 Environment 500-501, 250-269.
543 Wang, P., He, Y.-L.Huang, C.-H., 2010. Oxidation of fluoroquinolone antibiotics and
544 structurally related amines by chlorine dioxide: Reaction kinetics, product and
545 pathway evaluation. Water Research 44(20), 5989-5998.
546 Wang, Z., Bush, R.T., Sullivan, L.A., Chen, C.Liu, J., 2014. Selective Oxidation of Arsenite
547 by Peroxymonosulfate with High Utilization Efficiency of Oxidant. Environmental
548 Science & Technology 48(7), 3978-3985.
549 Wols, B.A., Harmsen, D.J.H., Wanders-Dijk, J., Beerendonk, E.F.Hofman-Caris, C.H.M.,
550 2015. Degradation of pharmaceuticals in UV (LP)/H2O2 reactors simulated by means
551 of kinetic modeling and computational fluid dynamics (CFD). Water Research 75, 11-
552 24.
553 Xu, Y., Liu, S., Guo, F.Zhang, B., 2016. Evaluation of the oxidation of enrofloxacin by
554 permanganate and the antimicrobial activity of the products. Chemosphere 144, 113-
555 121.
556 Yang, B., Kookana, R.S., Williams, M., Ying, G.-G., Du, J., Doan, H.Kumar, A., 2016a.
557 Oxidation of ciprofloxacin and enrofloxacin by ferrate(VI): Products identification,
558 and toxicity evaluation. Journal of Hazardous Materials 320, 296-303.

559 Yang, Y., Banerjee, G., Brudvig, G.W., Kim, J.-H.Pignatello, J.J., 2018. Oxidation of
560 Organic Compounds in Water by Unactivated Peroxymonosulfate. Environmental
561 Science & Technology 52(10), 5911-5919.
562 Yang, Y., Pignatello, J.J., Ma, J.Mitch, W.A., 2016b. Effect of matrix components on
563 UV/H2O2 and UV/S2O82− advanced oxidation processes for trace organic
564 degradation in reverse osmosis brines from municipal wastewater reuse facilities.
565 Water Research 89, 192-200.
566 Yin, R., Guo, W., Wang, H., Du, J., Zhou, X., Wu, Q., Zheng, H., Chang, J.Ren, N., 2018.
567 Selective degradation of sulfonamide antibiotics by peroxymonosulfate alone: Direct
568 oxidation and nonradical mechanisms. Chemical Engineering Journal 334, 2539-2546.
569 Yun, E.-T., Lee, J.H., Kim, J., Park, H.-D.Lee, J., 2018. Identifying the Nonradical
570 Mechanism in the Peroxymonosulfate Activation Process: Singlet Oxygenation
571 Versus Mediated Electron Transfer. Environmental Science & Technology 52(12),
572 7032-7042.
573 Yun, E.-T., Yoo, H.-Y., Bae, H., Kim, H.-I.Lee, J., 2017. Exploring the Role of Persulfate in
574 the Activation Process: Radical Precursor Versus Electron Acceptor. Environmental
575 Science & Technology 51(17), 10090-10099.
576 Zhang, H.Huang, C.-H., 2005. Oxidative Transformation of Fluoroquinolone Antibacterial
577 Agents and Structurally Related Amines by Manganese Oxide. Environmental
578 Science & Technology 39(12), 4474-4483.
579 Zhang, T., Chen, Y.Leiknes, T., 2016. Oxidation of Refractory Benzothiazoles with
580 PMS/CuFe2O4: Kinetics and Transformation Intermediates. Environmental Science
581 & Technology 50(11), 5864-5873.
582 Zhang, T., Zhu, H.Croué, J.P., 2013. Production of sulfate radical from peroxymonosulfate
583 induced by a magnetically separable CuFe2O4 spinel in water: Efficiency, stability,
584 and mechanism. Environmental Science and Technology 47(6), 2784-2791.
585 Zhou, Y., Gao, Y., Pang, S.-Y., Jiang, J., Yang, Y., Ma, J., Yang, Y., Duan, J.Guo, Q., 2018.
586 Oxidation of fluoroquinolone antibiotics by peroxymonosulfate without activation:
587 Kinetics, products, and antibacterial deactivation. Water Research 145, 210-219.

588

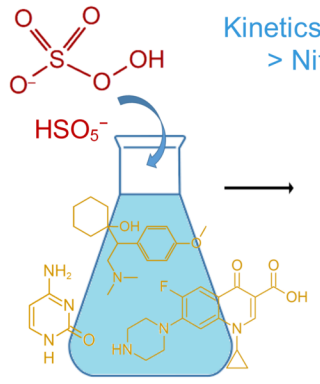

Nitrogenous Compounds

Kinetics: Piperazine moiety > Aliphatic amines
> Nitrogenous heterocyclic compounds

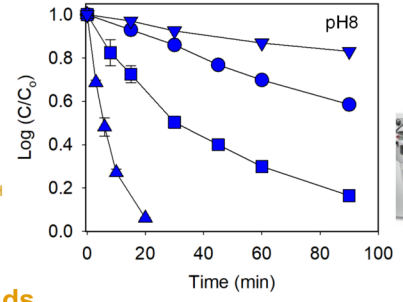

HRMS

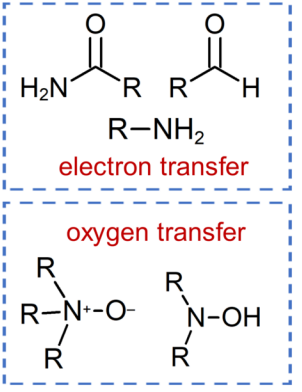

Transformation Products